Biogeosciences Discuss., doi:10.5194/bg-2016-533, 2017
Manuscript under review for journal Biogeosciences
Published: 9 January 2017

Biogeosciences Discussions Open Access EGU

Sediment phosphorus speciation and mobility under dynamic redox conditions

Chris T. Parsons[*1], *Fereidoun Rezanezhad*[1], *David W. O'Connell*[1,2], *Philippe Van Cappellen*[1]

[1]Ecohydrology Research Group and The Water Institute, University of Waterloo, 200 University Avenue West, Waterloo, Ontario, Canada.

[2]Department of Civil, Structural and Environmental Engineering, Trinity College Dublin, College Green, Museum Building, Dublin 2, Ireland.

[*]Corresponding author: Chris.Parsons@uwaterloo.ca

KEYWORDS: phosphorus, eutrophication, internal loading, redox cycling, bioturbation

ABSTRACT

Anthropogenic nutrient enrichment has caused phosphorus (P) accumulation in many freshwater sediments, raising concerns that internal loading from legacy P may delay the recovery of aquatic ecosystems suffering from eutrophication. Benthic recycling of P strongly depends on the redox regime at the sediment-water interface (SWI) that, in many shallow environments, tends to be highly dynamic as a result of, among others, bioturbation by macrofauna, root activity, sediment resuspension and seasonal variations in bottom water oxygen (O_2)

Biogeosciences Discuss., doi:10.5194/bg-2016-533, 2017
Manuscript under review for journal Biogeosciences
Published: 9 January 2017

concentrations. To gain insight into the mobility and biogeochemistry of P under fluctuating redox conditions, a suspension of sediment from a hyper-eutrophic freshwater marsh was exposed to alternating 7-day periods of purging with air and nitrogen gas (N_2), for a total duration of 74 days. At the start of each anoxic period, algal necromass was added to simulate the deposition of fresh autochtonous organic matter. Phosphatase activities up to 2.4 mmol h^{-1} kg^{-1} indicated the potential for rapid mineralization of added organic-P (P_o), in particular during the periods of aeration when the activity of phosphomonoesterases was up to 37% higher than under N_2 sparging. Aqueous phosphate concentrations remained low (~2.5 μM) under oxic conditions, due to sorption to Fe/Mn-oxides. During anoxic periods, once nitrate was depleted, the reductive dissolution of Fe/Mn-oxides released P. However, only 4.5% of the released P accumulated in solution while the rest was redistributed among the particulate phases, including the humic fraction. Thus, under the relatively short-term redox fluctuations imposed in the experiments, P remobilization to the aqueous phase remained relatively limited and poly-phosphate did not accumulate. The results also emphasize the important control bottom water nitrate concentrations may exert on internal P loading in eutrophic environments.

Keywords:
^{31}P NMR, sequential extractions, coupled biogeochemical cycling, phosphorus, iron, sulfur, redox oscillation, redox fluctuation, bioreactor

Biogeosciences Discuss., doi:10.5194/bg-2016-533, 2017
Manuscript under review for journal Biogeosciences
Published: 9 January 2017

INTRODUCTION

It is widely recognized that accelerated eutrophication of aquatic environments is caused primarily by anthropogenic increases to dissolved phosphorus (P) concentrations in surface water (Smith and Schindler, 2009). Rapid cultural eutrophication of oligo or mesotrophic lacustrine and palustrine systems is often attributed to increased external P loadings originating in agricultural run-off and waste water treatment plant (WWTP) effluent. The resultant excessive algal growth negatively impacts aquatic ecosystems and economic activity (Pretty et al., 2003), as well as increasing the risk of infectious diseases (Chun et al., 2013). Strategies to mitigate eutrophication have aimed to reduce point source and diffuse external phosphorus loadings by instituting agricultural best management practices in the surrounding watershed (McLaughlin and Pike, 2014; Sharpley et al., 1994), limiting P inputs to domestic waste water (Corazza and Tironi, 2011) and upgrading WWTPs (Mallin et al., 2005). However, internal loading of P, from sediments to surface water, remains poorly quantified in many systems, and is often the largest source of error in hydrodynamic and ecological phosphorus models (Kim et al., 2013). Early diagenesis and mineralogical removal of labile autochthonous organic phosphorus (P_o) from solution is a complex process and is poorly understood in highly dynamic systems despite exerting a strong influence on the magnitude of internal P loading. This is particularly true in shallow lakes and wetlands due to the high sediment surface area to water column depth ratio (Søndergaard et al., 2003).

As policy and infrastructure improvements continue in order to mitigate external P inputs to aquatic systems, the relative importance of internal P loads from legacy P in sediments to overall P budgets in eutrophic systems is likely to increase (Reddy et al., 2011).

Biogeosciences Discuss., doi:10.5194/bg-2016-533, 2017
Manuscript under review for journal Biogeosciences
Published: 9 January 2017

It has been widely demonstrated through laboratory and field investigations, particularly in seasonally anoxic lakes, that sustained anoxic conditions induced by water column stratification, typically result in greater P mobility, and correspondingly higher water column P concentrations (D. Krom and A. Berner, 1981; Hongve, 1997; Katsev et al., 2006; Mortimer, 1971, 1941; Penn et al., 2000). The microbially mediated reductive dissolution of these phases during sustained periods of anoxia at the sediment water interface (SWI) is often considered to be the main mechanism responsible for P release under anoxic conditions.

However, redox conditions in shallow, heavily bioturbated sediments are more spatially and temporally variable than in seasonally anoxic lakes (Aller, 1994; Gorham and Boyce, 1989) resulting in short term redox oscillations even with continuous oxia at the SWI.

Additionally, the coupled biogeochemical cycles of other redox sensitive elements, such as sulfur (Gächter and Müller, 2003) and carbon (Joshi et al., 2015; Katsev et al., 2006) have been shown to play important and complex roles in phosphorus mobility (O'Connell et al., 2015). Degradation of P_o can be slow below the SWI in lakes (Reitzel et al., 2007), occurring on timescales of years (Ahlgren et al., 2005) resulting in the accumulation and burial of P_o in sediments of hyper eutrophic lakes. P accumulation within microbial biomass in surface sediments has also been highlighted (Hupfer et al., 2008, 1995; Turner et al., 2006) as has long term P_o retention in tropical wetland sediments (Turner et al., 2006) however the effects of near surface redox oscillations on P_o retention are not well understood.

The aim of this study is to elucidate the microbial and geochemical mechanisms of in sediment phosphorus cycling and release associated with commonly occurring short redox fluctuations (days) at the SWI in shallow eutrophic environments. Particularly, we aimed to determine if: 1) Polyphosphate cycling was observable within marsh sediments under redox oscillating

Biogeosciences Discuss., doi:10.5194/bg-2016-533, 2017
Manuscript under review for journal Biogeosciences
Published: 9 January 2017

83 conditions as has been shown in WWTP communities (Fu et al., 2009; Hupfer et al., 2007). 2)
84 The accumulation of autochthonous P_o species from algal necromass was an important P
85 immobilizing process in an example hyper-eutrophic shallow wetland system 3) Rates of P_o
86 degradation were a) affected by redox conditions and b) comparable to those reported in deeper
87 lake environments.
88 We conducted bioreactor experiments using sediment suspensions, designed to reproduce cyclic
89 redox conditions analogous to those occurring in nature (Aller, 2004, 1994). A combination of
90 aqueous chemistry (cations, anions, dissolved organic carbon (DOC), SRP) sediment extractions
91 (modified SEDEX protocol and TP), spectroscopy (solution ^{31}P NMR) and extra-cellular enzyme
92 assays, using 4-methylumbelliferyl (MUF) tagged substrates, were used to evaluate bulk
93 chemistry, microbial and mineralogical controls on mobility during reactor experiments.

94 # Methods

95 ## Field site and sampling

96 Surface sediment (0-12 cm), sediment cores (34 cm long, 10 cm diameter), overlying water and
97 green filamentous algae (GFA) were collected on September 5, 2013 from West Pond in Cootes
98 Paradise Marsh (43.26979N, 79.92899W) following established guidelines (U.S. EPA, 9/99).
99 Cootes Paradise is a hyper-eutrophic, coastal freshwater marsh, which drains into Lake Ontario
100 via Hamilton Harbour (see Figure 1A-1C). The marsh system, and particularly West Pond,
101 suffered severe degradation due to rapid urbanization, population growth and nutrient loadings in
102 the 20th century (Chow-Fraser et al., 1998). Sand filters were introduced to the Dundas WWTP,
103 which flows into West Pond, in 1987 to decrease P loading, but prior to this extremely high P
104 effluent entered the marsh continually for several decades (Painter et al., 1991). The addition of

Biogeosciences Discuss., doi:10.5194/bg-2016-533, 2017
Manuscript under review for journal Biogeosciences
Published: 9 January 2017

105 sand filters and further improvements decreased P loadings from the WWTP from 45 kg P day^{-1}
106 in the early 1970's (Semkin et al., 1976) to 4.5 kg P day^{-1} in the 1980s (Chow-Fraser et al., 1998)
107 and 2.59 kg P day^{-1} in 2011 (Routledge, 2012). However, high legacy P concentrations in
108 sediment (up to 6200 $\mu g\ g^{-1}$) in the 1980's (Theysmeyer et al., 1999) resulted in dredging in
109 order to remediate the most affected areas in 1999 in an attempt to reduce harmful green
110 filamentous algae blooms (Bowman and Theysmeyer, 2014)

111 Despite restoration efforts, pervasive growth of GFA during the summer persists in parts of
112 Cootes Paradise, including West Pond (Figure 1A). Cyanobacteria are not commonly observed at
113 this location, potentially due to the high N:P ratios often associated with WWTP with tertiary P
114 removal treatment (Conley et al., 2009; Stumm and Morgan, 1996).

115 **Sediment characterization**

116 Sediment cores were sliced every 3 cm, homogenized and characterized with bulk sediment
117 samples prior to bioreactor experiments. Organic carbon and carbonate fractions were
118 determined by thermo-gravimetric analysis (TGA-Q500, TA Instruments Q500) (Pallasser et al.,
119 2013). Further elemental composition (e.g. total phosphorus (TP)) was determined by ashing and
120 acidic dissolution (HCl) followed by Inductively Coupled Plasma Optical Emission
121 Spectrometry (ICP-OES, Thermo Scientific iCAP 6300). Water content and bulk density (ρ_b) of
122 the sliced sediment core were determined gravimetrically after oven drying (Gardner, 1986).
123 Crystalline mineralogy phase identification and quantification were determined by powder X-ray
124 diffraction (XRD) (Empyrean, PANalytical). The density of benthic macro-invertebrates was
125 also quantified by counting after sieving two additional 7.5 cm diameter, 18 cm deep cores
126 through 500 µm mesh.

Biogeosciences Discuss., doi:10.5194/bg-2016-533, 2017
Manuscript under review for journal Biogeosciences
Published: 9 January 2017

Bioreactor experiment and redox oscillation procedure

An initial, concentrated, sediment suspension of approximately 500 g L^{-1} (dry weight equivalent) was prepared from freshly sampled sediment (0-12 cm) and filtered overlying water (<0.45 μm). Surface water was used, rather than distilled water, to provide background ionic strength and avoid osmotic shock to the microbial community. The concentrated suspension was stirred vigorously for 5 minutes then passed through a <500 µm stainless steel sieve to remove larger solid organic material and macro-invertebrates. This procedure was repeated until a homogeneous suspension was achieved. The dry weight was then re-determined, and the sieved solution was diluted with filtered surface water to a final concentration of 247 ± 2 g L^{-1}. The resulting suspension was transferred to a bioreactor system (Applikon Biotechnology) after Thompson et al (Thompson et al., 2006) and Parsons et al (Parsons et al., 2013). In addition to affording precise temperature control and continuous logging of temperature, redox potential (E_h) and pH, the system offers significant advancements over previous designs (Thompson 2006, Guo 2007, Parsons 2013). The E_h, pH and DO were measured using a combined autoclavable Mettler Toledo InPro 3253i/SG open-junction electrode and an AppliSens Low drift polarographic sensor. The InPro electrode system, using a common reference electrode, was chosen to help avoid potential interference between two electrodes in close proximity. A multi parameter transmitter was used to display current pH, E_h and temperature, to automatically temperature correct pH values and to adjust measured E_h to the standard hydrogen electrode (SHE). Dissolved oxygen (DO) was calibrated using 100% saturation in air (approximately 0.2905 atm) and 0% saturation in N_2 at constant sparging of 30 ml min^{-1}

The suspension was stirred continuously and sparged with 30 mL min^{-1} air for 11 days to equilibrate prior to the redox oscillation procedure. During the 11 day oxic equilibration period,

Biogeosciences Discuss., doi:10.5194/bg-2016-533, 2017
Manuscript under review for journal Biogeosciences
Published: 9 January 2017

150 CO_2 emissions were monitored the reactor exhaust gas using an IR sensor (Applikon
151 Biotechnology).

152 Subsequently, redox potential (E_h) variation was induced by the modulation of sparging gases
153 (30 ml min^{-1}) between N_2:CO_2 and O_2:N_2:CO_2. The suspension was subjected to five cycles of
154 anoxia (7 days) and oxia (7 days) at constant temperature (25°C) in the dark, while recording E_h,
155 pH, DO and temperature data. The suspension was sampled on days 1, 3, 5 and 7 of each half-
156 cycle. To separate solid and aqueous components from the sediment suspension, syringe
157 extracted samples (15 ml) were centrifuged at 5000 rpm for 20 minutes and the supernatant
158 filtered through 0.45 µm polypropylene membrane filters prior to all aqueous analysis. For
159 samples taken during reducing cycles, centrifugation, filtering and subsampling were performed
160 in an anoxic glove box (N_2:H_2 97:3%, O_2 < 1 ppmv). Time periods were chosen to be
161 representative of short temporal fluctuations to redox conditions experienced by surficial
162 sediments (Aller, 1994; Nikolausz et al., 2008; Parsons et al., 2013). To avoid unrealistically
163 high depletion of labile organic matter (OM) not replaced by primary productivity during the
164 experiment, 3 g of freeze dried, ground, GFA were added to the suspension at the onset of each
165 anoxic cycle. The amount of algae added was determined based on the CO_2 production from the
166 reactor during the initial 11 day oxic period, to balance gaseous carbon and nitrogen losses due
167 to microbial metabolism and avoid depletion of labile organic carbon, which often results in a
168 slowdown of metabolic processes in laboratory based soil and sediment experiments (Parsons et
169 al., 2013).

170 **Aqueous phase methods**

171 All reagents used were of analytical grade from Fluka, Sigma-Aldrich or Merck unless stated
172 otherwise. All reagents were prepared with 18.2 MΩcm^{-1} water (Millipore). Total dissolved Na

Biogeosciences Discuss., doi:10.5194/bg-2016-533, 2017
Manuscript under review for journal Biogeosciences
Published: 9 January 2017

(70), K(100), Ca(20), Mg(0.5), Mn(1), Fe(3), Al(100), P (TDP (2)), Si (15) and S (15) concentrations (Method detection limit MDL in μg L^{-1}, in brackets) were determined by ICP-OES (Thermo Scientific iCAP 6300) after filtration (< 0.45 μm) and acidification with HNO_3 to < pH 2. Matrix-matched standards were used for all calibrations and NIST validated multi-elemental solutions were used as controls. SRP concentrations were determined by the molybdenum blue/ascorbic acid method on a LaChat QuickChem 8500 flow injection analyser system (*4500-P E: Phosphorus by Ascorbic Acid*, 1992; Murphy and Riley, 1962) (Method detection limit (MDL) 1.2 μg P L^{-1}). DOC was determined using a Shimadzu TOC-LCPH/CPN analyser (Shimadzu) following HCl addition (< pH 2) to degas dissolved inorganic carbon (DIC) (MDL 71 μg C L^{-1}).

Chloride, nitrate, nitrite and sulfate concentrations were measured by ion chromatography using a Dionex ICS 5000 equipped with a capillary IonPac® AS18 column. Aqueous sulfide was stabilized with 20 μL 1% zinc acetate per mL (Pomeroy, 1954) after filtering and determined by the the Cline method (Cline, 1969) (MDL 0.5 µM). $Fe^{2+}_{(aq)}$ was determined by the ferrozine method immediately after filtering (Stookey, 1970; Viollier et al., 2000) (MDL 3.8 μM). All aqueous analyses were conducted in triplicate. The precision and accuracy for all techniques was <5 RSD% and ±10% with respect to certified reference materials (where commercially available).

Solid phase methods: Phosphorus and Iron Speciation

Fe^{2+} generated by dissimilatory iron reduction has been shown to sorb to mineral surfaces in sediment (Gehin et al., 2007; Klein et al., 2010; Liger et al., 1999) or precipitate as ferrous carbonate (Jensen et al., 2002), ferrous sulfide or other mixed ferrous/ferric phases (Rickard and Morse, 2005). Total Fe^{2+} production during anoxic half-cycles was estimated by a partial

Biogeosciences Discuss., doi:10.5194/bg-2016-533, 2017
Manuscript under review for journal Biogeosciences
Published: 9 January 2017

196 extraction (1 hour, 0.5N HCl) on sampled suspensions. Fe^{2+}/Fe^{3+} ratios were determined in
197 extracts using a modification of the ferrozine method (Stookey, 1970; Viollier et al., 2000).

198 Phosphorus partitioning within the solid phase was evaluated by both sequential extractions,
199 using a modification (Baldwin, 1996) of the SEDEX extraction scheme (Ruttenberg, 1992) and
200 solution ^{31}P NMR spectroscopy (Cade-Menun, 2005). The two approaches are complementary;
201 ^{31}P NMR spectroscopy provides information on the molecular level speciation of phosphorus,
202 while extraction provides information on the association of the P species with solid phase
203 fractions.

204 The modification of the extraction scheme (Baldwin, 1996), adds a 1M $NaHCO_3$ step to
205 differentiate between P associated with metal-OM bridging complexes and truly reducible oxide
206 associated P. Without this modification Li et (Li et al., 2015) al have shown that CDB also
207 extracts fine oxide-OM-P complexes. The final extraction scheme distinguishes the following
208 fractions: Easily exchangeable (P_{Ex}, 1M $MgCl_2$), humic-bound (P_{Hum} 1M $NaHCO_3$), oxide bound
209 (P_{Fe}, CDB), $CaCO_3$ bound (P_{CFA}, 1M Acetate pH 4), detrital apatite/other inorganic P (P_{Detr}, 1M
210 HCl), organic-P (P_{Resi}, 1M HCl after ashing at 550 °C).

211 **NaOH-EDTA Extraction and Solution ^{31}P NMR Spectroscopy**

212 Phosphorus was extracted directly from suspension samples (~2 g dry weight equivalent) prior to
213 solution ^{31}P NMR. The method (Cade-Menun and Preston, 1996) has been shown to allow
214 quantitative analyses of P_o (monoester and diester), polyphosphates and orthophosphate
215 (Amirbahman et al., 2013; Cade-Menun et al., 2006, p.; Reitzel et al., 2007; Turner et al., 2003).
216 Briefly, Samples were extracted in 25 mL of 0.25 M (NaOH) and Na_2EDTA (0.05 M) at ambient
217 laboratory temperature (~22 °C) for 4 hours. Subsequently, the tubes were centrifuged (3500 rpm

Biogeosciences Discuss., doi:10.5194/bg-2016-533, 2017
Manuscript under review for journal Biogeosciences
Published: 9 January 2017

for 20 minutes) and the supernatant extracted via syringe then neutralized with 2M HCl to a pH of 7 to avoid the breakdown of polyphosphates during freeze drying (Cade-Menun et al., 2006). This solution was then filtered to 0.45 µm. Prior to freeze drying 1 mL aliquots of each supernatant were diluted and analysed by ICP-OES spectroscopy for Al, Ca, Fe, Mg, Mn and P. The remaining extracts were frozen at -80 ^{o}C and lyophilized for 48 hours. The lyophilized extracts were re-dissolved in 1.0 ml D_2O, 0.6 ml 10 M NaOH, and 0.6 ml of the NaOH-EDTA extractant solution and were allowed to stand for 10 min with occasional vortexing. Samples were centrifuged for 20 min at 3500 rpm, transferred to 10-mm NMR tubes, and stored at 4 °C before analysis within 12 hours.

Solution ^{31}P NMR spectra were obtained using a 600-MHz spectrometer equipped with a 10-mm broadband probe. The NMR parameters were: 90° pulse, 0.68-s acquisition time, 4.32-s pulse delay, 12 Hz spinning, 20 °C, 2200 to 2900 scans (3-4h) for 0-5cm sediment samples (Cade-Menun et al., 2010). Phosphorus compounds were identified by their chemical shifts related to an external orthophosphoric acid standard, with the orthophosphate peak in all spectra standardized to 6ppm. Peak areas were calculated by integration on spectra processed with 10 and 7-Hz line broadening, using NUTS software (Acorn NMR, Livermore CA, 2000 edition). Peak assignments were grouped into compounds or groups of specific compound classes if direct identifications could not be made (Cade-Menun, 2005).

Extracellular enzyme assays

Rates of enzymatic hydrolysis of P_o were estimated through extracellular enzyme activities (EEA). Degradation rates for phosphomonoesters, phosphodiesters and pyrophosphate were determined fluorometrically through use of the MUF tagged substrates; MUF phosphate (MUP), Bis(MUF)phosphate (DiMUP, Chem-Impex International), and MUF pyrophosphate, (PYRO-P),

Biogeosciences Discuss., doi:10.5194/bg-2016-533, 2017
Manuscript under review for journal Biogeosciences
Published: 9 January 2017

241 Chem-Impex International) respectively. Additionally MUF β-D-glucopyranoside (MUGb) was
242 used in order to compare phosphatase enzyme activity to the activity of β-glucosidase (cellulase)
243 (Dunn et al., 2013). Enzyme activities were determined using a microplate reader (Flexstation3,
244 Molecular Devices) using a modification of Deng et al (Deng et al., 2013). Briefly, 1 g dry
245 weight equivalent of suspension from the reactor was stirred with 100 mL of 100mM HEPES
246 buffer at pH 7.5 in a pyrex dish for 10 minutes at 280 rpm to allow for complete homogenization.
247 Subsamples (100 µL) of the buffered soil suspension were removed during continuous mixing
248 using a multi-channel pipette and placed into microplate wells, which were loaded into the
249 microplate reader. Four replicate wells were filled per substrate. Plates were left to equilibrate
250 at 30 ^{o}C for 5 minutes inside the reader before the automatic addition of 100 µL of substrate,
251 resulting in a final substrate concentration of 667 µM. Each well was triturated thoroughly
252 during addition of the substrate. Excitation fluorescence was set at 365 nm was subsequently
253 recorded 6 times at 450 nm at 5 minute intervals over a 6 hour period. The effect of fluorescence
254 quenching was accounted for in each sample by preparing MUF calibration curves in the same
255 soil suspension as used for the analysis. The limit of detection was determined to be 1.1 µM
256 MUF and the limit of quantification to be 3.3 µM (MUF), equivalent to 1.1 µM of phosphate for
257 the determination of phosphomonoesterase activities.

258 ## Results & Discussion

259 ### Sediment characterisation and evidence of bioturbation

260 Characterisation of sediment cores revealed physical and chemical solid phase homogeneity
261 within 0-10 cm, with a bulk density of ~1.3 g cm^{-3}, water content of ~50% (by weight), OM of
262 ~3% and a carbonate of ~25% (Figure 2B). Between 10 and 15 cm increases in bulk density and

Biogeosciences Discuss., doi:10.5194/bg-2016-533, 2017
Manuscript under review for journal Biogeosciences
Published: 9 January 2017

263 decreases to the sediment water content, OM % and carbonate fraction occur as soft sediment
264 transitions to clay.

265 Benthic macroinvertebrate density of approximately 49,500 individuals per m^2 is consistent with
266 previously reported densities of 50,000 individuals per m^2 (Pelegri and Blackburn, 1995). The
267 community composition is shown in Figure 2A. The community was dominated by aquatic
268 earthworms (*Tubificidae 60%* and *Branchiura sowerbyii 8%*) which typically feed and mix
269 sediment within the top 5-10 cm (Fisher et al., 1980; McCall and Fisher, 1980). Other groups
270 identified include *Ceratopogonidae* (No see ums or biting midges, 22%) including *Sphareomias*,
271 *Probezzia* and *Bezzia, Chironomidae* (Midges, 6%) including *Cryptochironomus* and *Tanypus,*
272 *Nemotoda* (round worms which were not further identified, 4%) and a single *Hyalella azteca*
273 (scud <1%).

274 Bioturbating organisms have previously been shown to alter biogeochemical cycling within
275 surface sediments (Hölker et al., 2015) by increasing solute fluxes (Furukawa et al., 2001;
276 Matisoff and Wang, 1998), increasing mixing of solid sediment (Fisher et al., 1980) and
277 bioconveying sediment particles (Lagauzère et al., 2009). These processes have been shown to
278 enhance sediment oxygen demand (McCall and Fisher, 1980; Pelegri and Blackburn, 1995),
279 enhance degradation of OM (Aller, 1994), increase rates of denitrification, increase transport of
280 contaminants to surface water (Lagauzère et al., 2009), and increase temporal fluctuation of
281 redox conditions (Aller, 1994). Efficient sediment mixing allows frequent re-oxidation of
282 reduced sediments and therefore regeneration of terminal electron acceptors (TEAs) (Furukawa
283 et al., 2001) such as nitrate, ferric iron and sulfate, which often limit mineralisation of OM in
284 sediments underlying hypereutrophic water bodies (Reddy and DeLaune, 2008). Electron donors
285 in the form of fresh autochthonous necromass are also rapidly redistributed vertically within the

Biogeosciences Discuss., doi:10.5194/bg-2016-533, 2017
Manuscript under review for journal Biogeosciences
Published: 9 January 2017

zone of bioturbation. This environment should therefore support a metabolically diverse and highly active microbial community (DeAngelis et al., 2010).

XRD analysis of the top 12 cm of sediment (Figure 2C) showed close agreement with the carbonate fraction determined by TGA (~25% by TGA vs 27% by XRD) indicating a calcite dominated, carbonate buffered system. The remaining mineral assemblage was dominated by quartz and clay minerals (Illite, 30% and Chamosite, 2%). No pyrite or vivianite was detected by XRD suggesting either their absence or presence in low abundance with poorly crystalline structures.

Experimental redox oscillation: Aqueous chemistry

E_h within the bioreactor oscillated between +470 and -250 mV (Figure 3) consistent with E_h ranges of wetland sediments (Nikolausz et al., 2008). In contrast, pH conditions within the sediment suspension remained constant between 7.2 and 7.5 for the duration of the experiment, consistent with calcite/dolomite buffered sediment, as identified via XRD analyses, at p_{CO2} of ~$10^{-1.8}$ atm. This range of E_h/pH conditions implies transitions across the thermodynamically predicted stability boundaries for multiple redox couples e.g. MnO_2/Mn^{2+}, $NO_3^-/NO_2^-/NH_4^+$, $FeOOH/Fe^{2+}$, SO_4^{2-}/HS^-, during each 14 day redox cycle. The upper E_h values recorded during oxic cycles are significantly lower than predicted by the O_2/H_2O couple (820 mV @ pH 7) but are consistent with the O_2/H_2O_2 couple (300 mV @ pH 7) which is considered to control electrode measured E_h under oxic conditions (Stumm and Morgan, 1996).

Aqueous chemistry data, shown in Figure 3, demonstrate the consumption of TEAs in order of decreasing nominal energetic yield, coupled to the oxidation of labile OM. Upon physical removal and consumption of residual oxygen by the aerobic respiration, nitrate concentration

Biogeosciences Discuss., doi:10.5194/bg-2016-533, 2017
Manuscript under review for journal Biogeosciences
Published: 9 January 2017

began to decrease in the solution. Decreases to nitrate concentration coincide with peaks of nitrite concentration within the first hour of oxygen removal, indicating microbial denitrification. Subsequent increases to $Mn_{(aq)}$, $Fe^{2+}_{(aq)}$ and $HS^{-}_{(aq)}$ are indicative of the reduction of MnO_2, FeOOH and SO_4^{2-} as more energetically efficient electron acceptors become depleted. The timing of the appearance of $Mn_{(aq)}$ (presumably as Mn^{2+} due to the low solubility of tri and tetravalent Mn) and Fe^{2+} to solution varies between cycles, appearing earlier within each subsequent anoxic cycle, however the apparent order of reduction remained consistent between all five redox cycles (O_2, NO_3^-, NO_2^-, MnO_2, FeOOH, SO_4^{2-}).

Relatively low concentrations of Fe^{2+} were measured in solution (up to 71 μM) but 0.5 M HCl extractions reveal that significantly more Fe^{2+} was produced within each anoxic cycle. Within the 0.5M HCl extractable solid phase, changes to Fe^{2+} concentration of 50 to 70 μmol g^{-1} occurred during each anoxic cycle, equivalent to between 12.35 and 17.29 mM of iron reduction within the reactor as a whole. Assuming that the difference between Fe^{2+} concentrations in the 0.5 M HCl extractable fraction between the last sample of the preceding oxic cycle and the last sample of the subsequent anoxic cycle are equivalent to total iron reduction, only approximately 0.63% of microbially reduced Fe^{2+} is measureable in solution. Although iron reduction varied between 50 and 70 μmol g^{-1} between cycles, the relative proportion of $Fe^{2+}_{(aq)}$ remained low at 0.63 +/- 0.4%. No significant cumulative change to Fe^{2+}/Fe^{3+} occurred over the course of the experiment indicating that solid phase Fe redox cycling was reversible, potentially due to rapid solid Fe^{2+} oxidation in the presence of O_2 and carbonate (Caldeira et al., 2010).

DOC concentrations, shown in Figure 3, fluctuated with redox conditions with higher concentrations occurring during anoxic conditions. DOC may be replenished by both enzymatic hydrolysis of particulate organic matter (POM) (Vetter et al., 1998) and desorption of mineral

Biogeosciences Discuss., doi:10.5194/bg-2016-533, 2017
Manuscript under review for journal Biogeosciences
Published: 9 January 2017

331 associated OM (Grybos et al., 2009). The addition of algal matter at the beginning of anoxic
332 cycles resulted in observable sharp peaks of DOC which was rapidly removed from solution,
333 probably due to a combination of mineralisation of labile DOC to HCO_3^- and sorption processes
334 (Chorover and Amistadi, 2001; Grybos et al., 2009). The peak of DOC supplied by addition of
335 algal matter represents mostly labile DOC, which is readily mineralised in comparison to the
336 residual organic matter, which persists in the system throughout the experiment. The
337 differences in humified OM mobility between oxic and anoxic cycles are unlikely to be due to
338 oxide dissolution as differences to DOC concentration are observed prior to increases in $Mn_{(aq)}$
339 and $Fe_{(aq)}$ concentrations in solution. We therefore postulate that solubility changes to humified
340 DOC are driven by minor (+/- 0.3) pH changes between oxic and anoxic conditions caused by
341 changes in pCO_2 between oxic and anoxic conditions as previously shown by Grybos et al in
342 wetland sediments (Grybos et al., 2009).

343 Lowest aqueous phosphorus concentrations, shown in Figure 4, occurred during oxic cycles
344 (~2.5 to 3 μM) and increased dramatically during anoxic cycles to a maximum concentration of
345 50 to 60 μM per cycle 88% of which occurred as SRP. The range of TDP concentrations within
346 the aqueous phase of the reactor suspension are similar to those reported in situ at the site by
347 Mayer et al (Mayer et al., 2006). The timing of phosphorus release to the aqueous phase
348 corresponds with increasing concentrations of $Fe^{2+}_{(aq).}$ This is reflected in a strong positive
349 correlation between TDP and Fe concentrations ($n = 37$, $R^2 = 0.93$, $p < 0.0001$). This occurs only
350 after depletion of residual O_2, NO_3^- and NO_2^-, after increases to $Mn_{(aq)}$ and before increases to HS^-
351 $_{(aq)}$. The timing of P suggests an iron oxide control on phosphorus mobility and indicates that
352 complete nitrate depletion is necessary prior to phosphorus release to the aqueous phase.

Biogeosciences Discuss., doi:10.5194/bg-2016-533, 2017
Manuscript under review for journal Biogeosciences
Published: 9 January 2017

353 **Sequential chemical extractions and solid phase P partitioning**

354 Sequential extractions provide further evidence for a ferric (hydr)oxide control on aqueous P
355 concentrations (Figure 4). The sum of P concentrations from all sequential extractions (61 ± 5
356 μmol g^{-1}) was within 10% of a total extraction (57 μmol g^{-1}). P was mostly associated with the
357 P_{Hum} (~26%) and P_{Fe} (~24%) fractions. Lower P concentrations were found in the P_{Ex} ~16%, P_{CFA}
358 ~15%, P_{Detr} ~12% and P_{Res} ~7% fractions.
359 Although only ~24% of TP was associated with the CDB extractable pool (P_{Fe}). The P_{Fe} fraction
360 shows greater inter-cycle variability than other solid phase P pools and is the only P pool in
361 which concentration consistently decreased during anoxic conditions and increased during oxic
362 conditions. Notably the calcium bound (P_{CFA}) pool exhibited no P im/mobilization behaviour due
363 to changes in redox conditions. When a P mass balance (Figure 5) is attempted to account for
364 increases to aqueous phosphorus (P_{Aq}) from the iron bound (P_{Fe}) pool during anoxic periods it
365 becomes evident that only approximately 4.5% of variability observed in the P_{Fe} pool (total P_{Fe}
366 variation of up to 4.5 μmol g^{-1} during anoxic periods) is necessary to account for the changes to
367 inter-cycle P_{Aq} concentrations (50 μM). The remainder of the P_{Fe} lost during anoxic cycles
368 appears to be reversibly redistributed to the P_{Ex} (~30%) and P_{Hum} (~65%) pools. The lack of
369 significant P_{Resi} (~7%) despite consistently high primary productivity in the sampling location
370 may suggest that P_o additions are rapidly degraded and do not accumulate annually. However, it
371 has been shown that P from fresh algal biomass may be released during the first extraction step
372 of the SEDEX protocol (P_{Ex}) (Ruttenberg, 1992), this fraction is also relatively minor compared
373 to total P concentrations (~16%). The P contribution from individual algal additions (~1.5 μmol
374 P g^{-1}) was relatively small compared to the total P mass in the reactor (61 μmol P g^{-1}) and within
375 the margin of analytical error associated with solid extractions. Additionally, no single fraction

Biogeosciences Discuss., doi:10.5194/bg-2016-533, 2017
Manuscript under review for journal Biogeosciences
Published: 9 January 2017

shows a clear increase over the course of the experiment, therefore quantification of the redistribution of added P is not possible.

Fe:P ratios

Sequential extraction data shown in Figure 4, aqueous chemistry data shown in Figure 3, and the correlation between aqueous Fe and P ($n = 37$, $R^2 = 0.93$, $p < 0.0001$) that phosphorus released to solution under anoxic conditions likely originated in the P_{Fe} pool. Although the maximum molar ratio for phosphate incorporation within ferric oxides has been shown to be 2:1 (Fe:P) (Thibault et al., 2009), it has been suggested that much higher solid Fe:P of 15 (Jensen et al., 1992) to >20 (Phillips et al., 1994) maybe necessary to control phosphorus mobility under oxic conditions. Results from bioreactor experiments suggest that phosphorus is retained in the solid phase under oxic conditions at total Fe:P ratios of just 4.1:1, potentially due to the association of P with other sedimentary pools, particularly P_{Hum}. Fe:P ratios below the stoichiometric limitation of 2:1, measured in the aqueous phase (1.5 to 1.9), during anoxic conditions are therefore likely due to the removal of Fe^{2+} from solution by secondary sorption and precipitation processes, subsequent to reductive dissolution. Probable secondary Fe^{2+} removal processes include the formation of amorphous FeS and sorption of Fe^{2+} to clays. This is supported by increases to Fe^{2+}/Fe^{3+} ratios in the 0.5 M HCl extractable fraction during anoxic conditions. Although considerable fresh precipitation of FeS is likely to have occurred during anoxic conditions, due to frequent reoxidation prevents permanent Fe removal in this system as has been demonstrated previously in lake sediments (Gächter and Müller, 2003).

Biogeosciences Discuss., doi:10.5194/bg-2016-533, 2017
Manuscript under review for journal Biogeosciences
Published: 9 January 2017

396 **P associated with OM (P_{Hum})**

397 It has been demonstrated that humic acids may compete with orthophosphate for surface binding
398 sites on various minerals including goethite (Sibanda and Young, 1986) and poorly ordered Fe
399 oxides (Gerke, 1993) in the short term, but that sorption of natural OM to freshly precipitated Fe
400 oxides may increase the long term sorption capacity of ferric oxide phases towards P by
401 decreasing recrystallization over time (Gerke, 1993) and by the formation of OM-Fe complexes
402 (Gerke, 1993). As spectroscopic characterisation of the P associated with the operationally
403 defined P_{Hum} fraction was not performed, this pool is considered to contain OM associated P of
404 unknown chemical speciation. Previous studies have provided evidence for ternary complexes
405 between ferric iron, OM and phosphate and that complexed ferric iron can increase the sorption
406 capacity of OM to greater than that of ferric iron in the form of ferrihydrite (Kizewski et al.,
407 2010b). Recent spectroscopic evidence for mixed Fe(III)-OM-phosphate (Kizewski et al.,
408 2010a) and Fe(III)-OM-arsenate (Mikutta and Kretzschmar, 2011; Sharma et al., 2010)
409 complexes also indicate that various Fe(III)-OM-phosphate structures are likely to be an
410 environmentally relevant form of P. We consider that the P_{Hum} pool is likely to represent a
411 variety of OM associated P likely coordinated with ferric iron, but potentially also with Ca and
412 Al, which may itself be associated with various mineral surfaces within the sediment. Sequential
413 extractions indicate that the P_{Hum} fraction is the most important P fraction in the investigated
414 sediment under all redox conditions and that reversible re-partitioning between this and the P_{Fe}
415 fraction occurs during redox condition changes, potentially due to release of occluded Fe(III)-
416 OM-P within Fe oxides during reductive dissolution.

Biogeosciences Discuss., doi:10.5194/bg-2016-533, 2017
Manuscript under review for journal Biogeosciences
Published: 9 January 2017

Hydrolytic enzyme activities

The activities of model phosphomonoesterases, phosphodiesterases and pyrophosphatase were higher under oxic conditions compared to anoxic conditions by 37% ($p < 0.005$), 8% (not significant) and 24% ($p = 0.08$) respectively. Phosphomonoesterases were found to have the highest activities despite the inherent overestimation of phosphodiesterase activities when using MUF tagged substrates (Sirová et al., 2013). The opposite trend was observed for glycopyranoside, part of the cellulose degradation pathway (Dunn et al., 2013), which showed consistently higher activity (69% $p = <0.05$) under anoxic conditions. The different trends exhibited by cellulose and phosphatase enzymes, indicates that changes in activity were not universal but specific to enzyme function. Phosphomonoesterase activities obtained in the current study (1.76 to 2.4 mmol h^{-1} kg^{-1}) are similar to those previously reported in wetland sediments (Kang and Freeman, 1999) however, direct rate comparisons cannot be made due to different analysis conditions and the use of sediment suspensions in the current study. Lowering of the water table in wetlands has been shown to increase the activity of phosphatase enzymes and the hydrolysis of P_o species (Song et al., 2007). However, water table fluctuation results in changes to moisture content and changes to redox conditions simultaneously preventing isolation of the causal variable in field investigations (Rezanezhad et al., 2014). We postulate that under anoxic conditions when phosphorus availability in the aqueous phase is high, production of extracellular phosphatase enzymes by the microbial community is down-regulated. Alternatively, when bioavailable phosphorus is removed from solution under oxic conditions, extracellular phosphatase production is up-regulated in response. Adjustments to enzyme production in response to changes in phosphate availability occur on short timescales (hours/days) for such trends to be observable during the experiment. An inverse relationship between phosphatase

Biogeosciences Discuss., doi:10.5194/bg-2016-533, 2017
Manuscript under review for journal Biogeosciences
Published: 9 January 2017

activities and phosphate concentration, has previously been shown spatially in wetlands by Kang and Freeman (Kang and Freeman, 1999) but to our knowledge never temporally in sediments.

^{31}P NMR

Results from ^{31}P NMR analyses (Figure 6) show that the majority of phosphorus was present in the solid phase as ortho-phosphate (84-91%) with 4-8% monoester P, 3-8% diester P and <1% phosphonates and polyphosphates with no clear trend in relative abundance emerging during the experiment despite algal additions. Therefore P_o did not represent a significant sink of P in the sampled sediment or as a result of experimental conditions. A higher mean monoester/diester ratio (2.31) was found in reduced samples than oxidised samples (0.97) a statistically significant difference ($p=0.04$). This difference could indicate that monoester P was either less efficiently extracted under oxic conditions due to sorption to metal oxides or that monoesterase/diesterase activity decreased under anoxic conditions, which is consistent with enzymatic activity assays (Figure 6). Total P_o determined by ^{31}P NMR varied between 9 and 16% over time compared to 5 to 11% in the P_{resi} from sequential extractions, indicating that not all P_o was extracted in the P_{resi} fraction, which is commonly referred to as the P_o fraction. We postulate that the remaining ~5% of total phosphorus, identified as P_o by ^{31}P NMR was extracted during previous steps in the sequential extraction scheme. The relative activities of phosphatase enzymes appear to correlate with the relative abundances of P_o species identified by ^{31}P NMR e.g. Monoesters > Diesters > Pyro-P.

Significant polyphosphate (> 1%) was not detected by ^{31}P NMR during experiments. Previous studies focusing on WWTP tertiary treatment for phosphate removal suggest that redox oscillating conditions promote intracellular poly-P accumulation during aerobic conditions to be used as an energy store under anoxic conditions in order to uptake short chain fatty acids (SCFA)

Biogeosciences Discuss., doi:10.5194/bg-2016-533, 2017
Manuscript under review for journal Biogeosciences
Published: 9 January 2017

463 in the absence of an electron acceptor (Hupfer et al., 2007; Wentzel et al., 1991). Phosphate
464 uptake during aerobic conditions therefore requires P availability in excess of what is required
465 for growth and maintenance of the microbial community. However, phosphate availability under
466 aerobic conditions is limited by sorption and coprecipitation with iron oxides, assuming
467 sufficient Fe:P. The P requirements by the microbial community are also likely to be high
468 during the transition to aerobic conditions due to the availability of O_2 as an energetically
469 efficient electron acceptor and fermentation products (SCFA) further decreasing the probability
470 of polyphosphate accumulation. Additionally, polyphosphate accumulation and release has
471 shown to be inhibited by denitrification and sulfate reduction due to competition for short chain
472 fatty acids (Kortstee et al., 1994; Yamamoto-Ikemoto et al., 1994).

473 **Implications**

474 Our controlled laboratory simulation of highly dynamic redox conditions in eutrophic sediment
475 demonstrates the importance of coupling multiple elemental cycles (C, N, Fe, S, P) when
476 determining internal P loading potential and timing. Our results demonstrate that neither
477 aqueous or solid phase Fe:P ratios or even solid phase P_{Fe} quantification are good predictors of
478 potential P release to the water column under anoxic conditions, due to extensive redistribution
479 of both reduced Fe and associated P within the solid phase. We show that 99.4% of reduced Fe
480 and 95.5% of P_{Fe} are not released to the aqueous phase upon Fe reduction but reversibly
481 redistributed within the solid phase upon short periods of iron reduction. Additionally, the
482 apparent requirement for complete nitrate depletion prior to anoxia-promoted P release to the
483 aqueous phase has implications for the management of WWTP effluent. Our results suggest that
484 decreasing NO_3^- concentrations in WWTP effluent, while ostensibly ecologically beneficial, may
485 increase the frequency and magnitude of internal P loading during short periods of anoxia. In P

Biogeosciences Discuss., doi:10.5194/bg-2016-533, 2017
Manuscript under review for journal Biogeosciences
Published: 9 January 2017

limited systems, the apparent benefits of decreased NO_3^- may be offset by increased P release and eutrophication. Finally, we demonstrate that oscillatory redox conditions, even in sediments with diverse and active microbial communities, do not necessarily result in accumulation of polyphosphate, ostensibly due to mineralogical phosphate immobilization.

Funding Sources

We acknowledge funding from the Canadian Excellence Research Chair (CERC) program and the Water Institute at the University of Waterloo.

Acknowledgements

We would like to acknowledge the support of the Royal Botanical Gardens, particularly Jennifer Bowman and Tys Theymeyer as well as Taylor Maavara who kindly provided her pack raft for use during field sampling, Jia Cheng (Allen) Yu for his assistance with the production of Figure 1.

Abbreviations

Green filamentous algae; GFA, waste water treatment plants; WWTP, sediment-water interface; SWI, dissolved organic carbon; DOC, organic phosphorus species; P_o, soluble reactive phosphorus; SRP, Inductively Coupled Plasma Optical Emission Spectrometry; ICP-OES, organic matter; OM, powder X-ray diffraction; XRD, dissolved reactive phosphorus; DRP, Method detection limit; MDL, non-purgeable organic carbon; NPOC, total dissolved phosphorus; TDP, dissolved inorganic carbon; DIC, relative standard deviation; RSD%, 4-methylumbelliferyl; MUF, 4-Methylumbelliferyl phosphate; MUP, Bis(4-

506 methylumbelliferyl)phosphate; DiMUP, and 4-Methylumbelliferyl pyrophosphate; PYRO-P, 4-
507 Methylumbelliferyl beta-D-glucopyranoside; MUGb, thermo-gravimetric analysis; TGA,
508 terminal electron acceptors; TEAs, particulate organic matter; POM, total phosphorus; TP.

509 ## References

510 4500-P E: Phosphorus by Ascorbic Acid, 1992. , Standard Methods for the Examination of
511 Water and Wastewater. National Water Quality Monitoring Council, Washington, DC,
512 U.S.
513 Ahlgren, J., Tranvik, L., Gogoll, A., Waldebäck, M., Markides, K., Rydin, E., 2005. Sediment
514 Depth Attenuation of Biogenic Phosphorus Compounds Measured by ^{31} P NMR. Environ.
515 Sci. Technol. 39, 867–872. doi:10.1021/es049590h
516 Aller, R.C., 2004. Conceptual models of early diagenetic processes: The muddy seafloor as an
517 unsteady, batch reactor. J. Mar. Res. 62, 815–835. doi:10.1357/0022240042880837
518 Aller, R.C., 1994. Bioturbation and remineralization of sedimentary organic matter: effects of
519 redox oscillation. Chem. Geol. 114, 331–345. doi:doi: 10.1016/0009-2541(94)90062-0
520 Amirbahman, A., Lake, B.A., Norton, S.A., 2013. Seasonal phosphorus dynamics in the surficial
521 sediment of two shallow temperate lakes: a solid-phase and pore-water study.
522 Hydrobiologia 701, 65–77. doi:10.1007/s10750-012-1257-z
523 Baldwin, D.S., 1996. The phosphorus composition of a diverse series of Australian sediments.
524 Hydrobiologia 335, 63–73. doi:10.1007/BF00013684
525 Bowman, J., Theysmeyer, T., 2014. 2013 RBG Marsh Sediment Quality Assessment (No. Report
526 No. 2014-14). Royal Botanical Gardens, Burlington, Ontario.
527 Cade-Menun, B., 2005. Characterizing phosphorus in environmental and agricultural samples by
528 31P nuclear magnetic resonance spectroscopy. Talanta 66, 359–371.
529 doi:10.1016/j.talanta.2004.12.024
530 Cade-Menun, B.J., Carter, M.R., James, D.C., Liu, C.W., 2010. Phosphorus forms and chemistry
531 in the soil profile under long-term conservation tillage: a phosphorus-31 nuclear magnetic
532 resonance study. J. Environ. Qual. 39, 1647–1656.
533 Cade-Menun, B.J., Navaratnam, J.A., Walbridge, M.R., 2006. Characterizing Dissolved and
534 Particulate Phosphorus in Water with ^{31} P Nuclear Magnetic Resonance Spectroscopy.
535 Environ. Sci. Technol. 40, 7874–7880. doi:10.1021/es061843e
536 Cade-Menun, B.J., Preston, C.M., 1996. A Comparison of Soil Extraction Procedures for 31P
537 NMR Spectroscopy. Soil Sci. 161, 770–785. doi:10.1097/00010694-199611000-00006
538 Caldeira, C.L., Ciminelli, V.S.T., Osseo-Asare, K., 2010. The role of carbonate ions in pyrite
539 oxidation in aqueous systems. Geochim. Cosmochim. Acta 74, 1777–1789. doi:doi:
540 10.1016/j.gca.2009.12.014
541 Chorover, J., Amistadi, M.K., 2001. Reaction of forest floor organic matter at goethite, birnessite
542 and smectite surfaces. Geochim. Cosmochim. Acta 65, 95–109. doi:10.1016/S0016-
543 7037(00)00511-1
544 Chow-Fraser, P., Lougheed, V., Le Thiec, V., Crosbie, B., Simser, L., Lord, J., 1998. Long-term
545 response of the biotic community to fluctuating water levels and changes in water quality

in Cootes Paradise Marsh, a degraded coastal wetland of Lake Ontario. Wetl. Ecol. Manag. 6, 19–42. doi:10.1023/A:1008491520668

Chun, C.L., Ochsner, U., Byappanahalli, M.N., Whitman, R.L., Tepp, W.H., Lin, G., Johnson, E.A., Peller, J., Sadowsky, M.J., 2013. Association of Toxin-Producing *Clostridium botulinum* with the Macroalga *Cladophora* in the Great Lakes. Environ. Sci. Technol. 47, 2587–2594. doi:10.1021/es304743m

Cline, J.D., 1969. Spectrophotometric determination of hydrogen sulfide in natural waters. Limnol. Oceanogr. 14, 454–458. doi:10.4319/lo.1969.14.3.0454

Conley, D.J., Paerl, H.W., Howarth, R.W., Boesch, D.F., Seitzinger, S.P., Havens, K.E., Lancelot, C., Likens, G.E., 2009. ECOLOGY: Controlling Eutrophication: Nitrogen and Phosphorus. Science 323, 1014–1015. doi:10.1126/science.1167755

Corazza, C., Tironi, S., 2011. European Parliament supports ban of phosphates in consumer detergents (Press Release No. IP/11/1542). European Commission, Brussels, Belgium.

D. Krom, M., A. Berner, R., 1981. The diagenesis of phosphorus in a nearshore marine sediment. Geochim. Cosmochim. Acta 45, 207–216. doi:10.1016/0016-7037(81)90164-2

DeAngelis, K.M., Silver, W.L., Thompson, A.W., Firestone, M.K., 2010. Microbial communities acclimate to recurring changes in soil redox potential status. Environ. Microbiol. 12, 3137–3149. doi:10.1111/j.1462-2920.2010.02286.x

Deng, S., Popova, I.E., Dick, L., Dick, R., 2013. Bench scale and microplate format assay of soil enzyme activities using spectroscopic and fluorometric approaches. Appl. Soil Ecol. 64, 84–90. doi:10.1016/j.apsoil.2012.11.002

Dunn, C., Jones, T.G., Girard, A., Freeman, C., 2013. Methodologies for Extracellular Enzyme Assays from Wetland Soils. Wetlands 34, 9–17. doi:10.1007/s13157-013-0475-0

Fisher, J.B., Lick, W.J., McCall, P.L., Robbins, J.A., 1980. Vertical mixing of lake sediments by tubificid oligochaetes. J. Geophys. Res. 85, 3997. doi:10.1029/JC085iC07p03997

Fu, Z., Yang, F., An, Y., Xue, Y., 2009. Simultaneous nitrification and denitrification coupled with phosphorus removal in an modified anoxic/oxic-membrane bioreactor (A/O-MBR). Biochem. Eng. J. 43, 191–196. doi:10.1016/j.bej.2008.09.021

Furukawa, Y., Bentley, S.J., Lavoie, D.L., 2001. Bioirrigation modeling in experimental benthic mesocosms. J. Mar. Res. 59, 417–452. doi:10.1357/002224001762842262

Gächter, R., Müller, B., 2003. Why the Phosphorus Retention of Lakes Does Not Necessarily Depend on the Oxygen Supply to Their Sediment Surface. Limnol. Oceanogr. 48, 929–933. doi:10.2307/3096591

Gardner, W.H., 1986. Water Content, in: Methods of Soil Analysis: Physical and Mineralogical Methods, Agronomy. Soil Science Society of America, Madison, Wisconsin, pp. 493–544.

Gehin, A., Greneche, J.-M., Tournassat, C., Brendle, J., Rancourt, D.G., Charlet, L., 2007. Reversible surface-sorption-induced electron-transfer oxidation of Fe(II) at reactive sites on a synthetic clay mineral. Geochim. Cosmochim. Acta 71, 863–876. doi:doi: 10.1016/j.gca.2006.10.019

Gerke, J., 1993. Phosphate adsorption by humic/Fe-oxide mixtures aged at pH 4 and 7 and by poorly ordered Fe-oxide. Geoderma 59, 279–288. doi:10.1016/0016-7061(93)90074-U

Gorham, E., Boyce, F.M., 1989. Influence of Lake Surface Area and Depth Upon Thermal Stratification and the Depth of the Summer Thermocline. J. Gt. Lakes Res. 15, 233–245. doi:10.1016/S0380-1330(89)71479-9

591 Grybos, M., Davranche, M., Gruau, G., Petitjean, P., Pedrot, M., 2009. Increasing pH drives
592 organic matter solubilization from wetland soils under reducing conditions. Geoderma
593 154, 13–19. doi:doi: DOI: 10.1016/j.geoderma.2009.09.001
594 Hölker, F., Vanni, M.J., Kuiper, J.J., Meile, C., Grossart, H.-P., Stief, P., Adrian, R., Lorke, A.,
595 Dellwig, O., Brand, A., Hupfer, M., Mooij, W.M., Nützmann, G., Lewandowski, J., 2015.
596 Tube-dwelling invertebrates: tiny ecosystem engineers have large effects in lake
597 ecosystems. Ecol. Monogr. 85, 333–351. doi:10.1890/14-1160.1
598 Hongve, D., 1997. Cycling of iron, manganese, and phosphate in a meromictic lake. Limnol.
599 Oceanogr. 42, 635–647. doi:10.4319/lo.1997.42.4.0635
600 Hupfer, M., GäChter, R., RüEggger, H., 1995. Polyphosphate in lake sediments: 31P NMR
601 spectroscopy as a tool for its identification. Limnol. Oceanogr. 40, 610–617.
602 doi:10.4319/lo.1995.40.3.0610
603 Hupfer, M., Gloess, S., Grossart, H., 2007. Polyphosphate-accumulating microorganisms in
604 aquatic sediments. Aquat. Microb. Ecol. 47, 299–311. doi:10.3354/ame047299
605 Hupfer, M., Glöss, S., Schmieder, P., Grossart, H.-P., 2008. Methods for Detection and
606 Quantification of Polyphosphate and Polyphosphate Accumulating Microorganisms in
607 Aquatic Sediments. Int. Rev. Hydrobiol. 93, 1–30. doi:10.1002/iroh.200610935
608 Jensen, D.L., Boddum, J.K., Tjell, J.C., Christensen, T.H., 2002. The solubility of rhodochrosite
609 (MnCO3) and siderite (FeCO3) in anaerobic aquatic environments. Appl. Geochem. 17,
610 503–511. doi:doi: DOI: 10.1016/S0883-2927(01)00118-4
611 Jensen, H.S., Kristensen, P., Jeppesen, E., Skytthe, A., 1992. Iron:phosphorus ratio in surface
612 sediment as an indicator of phosphate release from aerobic sediments in shallow lakes.
613 Hydrobiologia 235–236, 731–743. doi:10.1007/BF00026261
614 Joshi, S.R., Kukkadapu, R.K., Burdige, D.J., Bowden, M.E., Sparks, D.L., Jaisi, D.P., 2015.
615 Organic Matter Remineralization Predominates Phosphorus Cycling in the Mid-Bay
616 Sediments in the Chesapeake Bay. Environ. Sci. Technol. 49, 5887–5896.
617 doi:10.1021/es5059617
618 Kang, H., Freeman, C., 1999. Phosphatase and arylsulphatase activities in wetland soils: annual
619 variation and controlling factors. Soil Biol. Biochem. 31, 449–454. doi:10.1016/S0038-
620 0717(98)00150-3
621 Katsev, S., Tsandev, I., L'Heureux, I., Rancourt, D.G., 2006. Factors controlling long-term
622 phosphorus efflux from lake sediments: Exploratory reactive-transport modeling. Chem.
623 Geol. 234, 127–147. doi:10.1016/j.chemgeo.2006.05.001
624 Kim, D.-K., Zhang, W., Rao, Y.R., Watson, S., Mugalingam, S., Labencki, T., Dittrich, M.,
625 Morley, A., Arhonditsis, G.B., 2013. Improving the representation of internal nutrient
626 recycling with phosphorus mass balance models: A case study in the Bay of Quinte,
627 Ontario, Canada. Ecol. Model. 256, 53–68. doi:10.1016/j.ecolmodel.2013.02.017
628 Kizewski, F.R., Boyle, P., Hesterberg, D., Martin, J.D., 2010a. Mixed Anion
629 (Phosphate/Oxalate) Bonding to Iron(III) Materials. J. Am. Chem. Soc. 132, 2301–2308.
630 doi:10.1021/ja908807b
631 Kizewski, F.R., Hesterberg, D., Martin, J., 2010b. Phosphate sorption to organic
632 matter/ferrihydrite systems as affected by aging time. Presented at the 19th World
633 Congress of Soil Science, Soil Solutions for a Changing World, Brisbane, Australia.
634 Klein, A.R., Baldwin, D.S., Singh, B., Silvester, E.J., 2010. Salinity-induced acidification in a
635 wetland sediment through the displacement of clay-bound iron(II). Environ. Chem. 7,
636 413. doi:10.1071/EN10057

637 Kortstee, G.J.J., Appeldoorn, K.J., Bonting, C.F.C., Niel, E.W.J., Veen, H.W., 1994. Biology of
638 polyphosphate-accumulating bacteria involved in enhanced biological phosphorus
639 removal. FEMS Microbiol. Rev. 15, 137–153. doi:10.1111/j.1574-6976.1994.tb00131.x
640 Lagauzère, S., Boyer, P., Stora, G., Bonzom, J.-M., 2009. Effects of uranium-contaminated
641 sediments on the bioturbation activity of Chironomus riparius larvae (Insecta, Diptera)
642 and Tubifex tubifex worms (Annelida, Tubificidae). Chemosphere 76, 324–334.
643 doi:10.1016/j.chemosphere.2009.03.062
644 Li, W., Joshi, S.R., Hou, G., Burdige, D.J., Sparks, D.L., Jaisi, D.P., 2015. Characterizing
645 Phosphorus Speciation of Chesapeake Bay Sediments Using Chemical Extraction, ^{31}P
646 NMR, and X-ray Absorption Fine Structure Spectroscopy. Environ. Sci. Technol. 49,
647 203–211. doi:10.1021/es504648d
648 Liger, E., Charlet, L., Van Cappellen, P., 1999. Surface catalysis of uranium(VI) reduction by
649 iron(II). Geochim. Cosmochim. Acta 63, 2939–2955. doi:doi: DOI: 10.1016/S0016-
650 7037(99)00265-3
651 Mallin, M.A., McIver, M.R., Wells, H.A., Parsons, D.C., Johnson, V.L., 2005. Reversal of
652 eutrophication following sewage treatment upgrades in the New River Estuary, North
653 Carolina. Estuaries 28, 750–760. doi:10.1007/BF02732912
654 Matisoff, G., Wang, X., 1998. Solute transport in sediments by freshwater infaunal bioirrigators.
655 Limnol. Oceanogr. 43, 1487–1499. doi:10.4319/lo.1998.43.7.1487
656 Mayer, T., Rosa, F., Mayer, R., Charlton, M., 2006. Relationship Between the Sediment
657 Geochemistry and Phosphorus Fluxes in a Great Lakes Coastal Marsh, Cootes Paradise,
658 ON, Canada. Water Air Soil Pollut. Focus 6, 495–503. doi:10.1007/s11267-006-9033-6
659 McCall, P.L., Fisher, J.B., 1980. Effects of Tubificid Oligochaetes on Physical and Chemical
660 Properties of Lake Erie Sediments, in: Brinkhurst, R., Cook, D. (Eds.), Aquatic
661 Oligochaete Biology. Springer US, pp. 253–317.
662 McLaughlin, C., Pike, K., 2014. Muddied Waters: The Ongoing Challenge of Sediment and
663 Phosphorus for Hamilton Harbour Remediation (2014 Towards Safe Harbour Report).
664 Bay Area Restoration Council, Hamilton, Ontario.
665 Mikutta, C., Kretzschmar, R., 2011. Spectroscopic Evidence for Ternary Complex Formation
666 between Arsenate and Ferric Iron Complexes of Humic Substances. Environ. Sci.
667 Technol. 45, 9550–9557. doi:10.1021/es202300w
668 Mortimer, C.H., 1971. Chemical Exchanges Between Sediments and Water in the Great Lakes-
669 Speculations on Probable Regulatory Mechanisms. Limnol. Oceanogr. 16, 387–404.
670 doi:10.2307/2834170
671 Mortimer, C.H., 1941. The exchange of dissolved substances between mud and water in lakes. J.
672 Ecol. 29, 280–329.
673 Murphy, J., Riley, J.P., 1962. A modified single solution method for the determination of
674 phosphate in natural waters. Anal. Chim. Acta 27, 31–36. doi:10.1016/S0003-
675 2670(00)88444-5
676 Nikolausz, M., Kappelmeyer, U., Szekely, A., Rusznyak, A., Marialigeti, K., Kastner, M., 2008.
677 Diurnal redox fluctuation and microbial activity in the rhizosphere of wetland plants. Eur.
678 J. Soil Biol. 44, 324–333. doi:doi: DOI: 10.1016/j.ejsobi.2008.01.003
679 O'Connell, D.W., Jensen, M.M., Jakobsen, R., Thamdrup, B., Andersen, T.J., Kovacs, A.,
680 Hansen, H.C.B., 2015. Vivianite formation and its role in phosphorus retention in Lake
681 Ørn, Denmark. Chem. Geol. doi:10.1016/j.chemgeo.2015.05.002

682 Painter, D.., Hampton, L., Simser, W.L., 1991. Cootes Paradise Water Turbidity: Sources and
683 Recommendations., in: NWRI Contribution Paper #91-15. Burlington, Ontario, p. 18.
684 Pallasser, R., Minasny, B., McBratney, A.B., 2013. Soil carbon determination by
685 thermogravimetrics. PeerJ 1, e6. doi:10.7717/peerj.6
686 Parsons, C.T., Couture, R.-M., Omoregie, E.O., Bardelli, F., Greneche, J.-M., Roman-Ross, G.,
687 Charlet, L., 2013. The impact of oscillating redox conditions: Arsenic immobilisation in
688 contaminated calcareous floodplain soils. Environ. Pollut. 178, 254–263.
689 doi:10.1016/j.envpol.2013.02.028
690 Pelegri, S.P., Blackburn, T.H., 1995. Effects of Tubifex tubifex (Oligochaeta: Tubificidae) on N-
691 mineralization in freshwater sediments, measured with isotopes. Aquat. Microb. Ecol. 9,
692 289–294.
693 Penn, M.R., Auer, M.T., Doerr, S.M., Driscoll, C.T., Brooks, C.M., Effler, S.W., 2000.
694 Seasonality in phosphorus release rates from the sediments of a hypereutrophic lake
695 under a matrix of pH and redox conditions. Can. J. Fish. Aquat. Sci. 57, 1033–1041.
696 doi:10.1139/f00-035
697 Phillips, G., Jackson, R., Bennett, C., Chilvers, A., 1994. The importance of sediment
698 phosphorus release in the restoration of very shallow lakes (The Norfolk Broads,
699 England) and implications for biomanipulation. Hydrobiologia 275–276, 445–456.
700 doi:10.1007/BF00026733
701 Pomeroy, R., 1954. Auxiliary Pretreatment by Zinc Acetate in Sulfide Analyses. Anal. Chem.
702 26, 571–572. doi:10.1021/ac60087a047
703 Pretty, J.N., Mason, C.F., Nedwell, D.B., Hine, R.E., Leaf, S., Dils, R., 2003. Environmental
704 Costs of Freshwater Eutrophication in England and Wales. Environ. Sci. Technol. 37,
705 201–208. doi:10.1021/es020793k
706 Reddy, K.R., DeLaune, R.D., 2008. Biogeochemistry of wetlands: science and applications.
707 CRC Press, Boca Raton.
708 Reddy, K.R., Newman, S., Osborne, T.Z., White, J.R., Fitz, H.C., 2011. Phosphorous Cycling in
709 the Greater Everglades Ecosystem: Legacy Phosphorous Implications for Management
710 and Restoration. Crit. Rev. Environ. Sci. Technol. 41, 149–186.
711 doi:10.1080/10643389.2010.530932
712 Reitzel, K., Ahlgren, J., DeBrabandere, H., Waldebäck, M., Gogoll, A., Tranvik, L., Rydin, E.,
713 2007. Degradation rates of organic phosphorus in lake sediment. Biogeochemistry 82,
714 15–28. doi:10.1007/s10533-006-9049-z
715 Rezanezhad, F., Couture, R.-M., Kovac, R., O'Connell, D., Van Cappellen, P., 2014. Water table
716 fluctuations and soil biogeochemistry: An experimental approach using an automated soil
717 column system. J. Hydrol. 509, 245–256. doi:10.1016/j.jhydrol.2013.11.036
718 Rickard, D., Morse, J.W., 2005. Acid volatile sulfide (AVS). Mar. Chem. 97, 141–197.
719 doi:10.1016/j.marchem.2005.08.004
720 Routledge, I., 2012. City of Hamilton: King Street (Dundas) Wastewater Treatment Plant. 2011
721 Annual Report (Annual Report No. Works Number 120001372). The City of Hamilton,
722 Environment and Sustainable Infrastructure Division, Hamilton, Ontario.
723 Ruttenberg, K.C., 1992. Development of a sequential extraction method for different forms of
724 phosphorus in marine sediments. Limnol. Oceanogr. 37, 1460–1482.
725 doi:10.4319/lo.1992.37.7.1460
726 Semkin, R.G., McLarty, A.W., Craig, D., 1976. A water quality study of Cootes Paradise.
727 Ontario Ministry of Environment, West Central Region, Toronto, Ontario.

728 Sharma, P., Ofner, J., Kappler, A., 2010. Formation of Binary and Ternary Colloids and
729 Dissolved Complexes of Organic Matter, Fe and As. Environ. Sci. Technol. 44, 4479–
730 4485. doi:10.1021/es100066s
731 Sharpley, A.N., Chapra, S.C., Wedepohl, R., Sims, J.T., Daniel, T.C., Reddy, K.R., 1994.
732 Managing Agricultural Phosphorus for Protection of Surface Waters: Issues and Options.
733 J. Environ. Qual. 23, 437. doi:10.2134/jeq1994.00472425002300030006x
734 Sibanda, H.M., Young, S.D., 1986. Competitive adsorption of humus acids and phosphate on
735 goethite, gibbsite and two tropical soils. J. Soil Sci. 37, 197–204. doi:10.1111/j.1365-
736 2389.1986.tb00020.x
737 Sirová, D., Rejmánková, E., Carlson, E., Vrba, J., 2013. Current standard assays using artificial
738 substrates overestimate phosphodiesterase activity. Soil Biol. Biochem. 56, 75–79.
739 doi:10.1016/j.soilbio.2012.02.008
740 Smith, V.H., Schindler, D.W., 2009. Eutrophication science: where do we go from here? Trends
741 Ecol. Evol. 24, 201–207. doi:10.1016/j.tree.2008.11.009
742 Søndergaard, M., Jensen, J.P., Jeppesen, E., 2003. Role of sediment and internal loading of
743 phosphorus in shallow lakes. Hydrobiologia 506–509, 135–145.
744 doi:10.1023/B:HYDR.0000008611.12704.dd
745 Song, K.-Y., Zoh, K.-D., Kang, H., 2007. Release of phosphate in a wetland by changes in
746 hydrological regime. Sci. Total Environ. 380, 13–18. doi:10.1016/j.scitotenv.2006.11.035
747 Stookey, L.L., 1970. Ferrozine - a new spectrophotometric reagent for iron. Anal. Chem. 42,
748 779–781. doi:doi: 10.1021/ac60289a016
749 Stumm, W., Morgan, J.J., 1996. Aquatic Chemistry, 3rd ed. ed. John Wiley & Sons, New York
750 [etc.].
751 Theysmeyer, T., Smith, T., Simser, L., 1999. West Pond 1999 Study. Royal Botanical Gardens,
752 Science Department.
753 Thibault, P.-J., Rancourt, D.G., Evans, R.J., Dutrizac, J.E., 2009. Mineralogical confirmation of
754 a near-P:Fe=1:2 limiting stoichiometric ratio in colloidal P-bearing ferrihydrite-like
755 hydrous ferric oxide. Geochim. Cosmochim. Acta 73, 364–376.
756 doi:10.1016/j.gca.2008.10.031
757 Thompson, A., Chadwick, O.A., Rancourt, D.G., Chorover, J., 2006. Iron-oxide crystallinity
758 increases during soil redox oscillations. Geochim. Cosmochim. Acta 70, 1710–1727.
759 doi:10.1016/j.gca.2005.12.005
760 Turner, B.L., Mahieu, N., Condron, L.M., 2003. Phosphorus-31 Nuclear Magnetic Resonance
761 Spectral Assignments of Phosphorus Compounds in Soil NaOH–EDTA Extracts. Soil
762 Sci. Soc. Am. J. 67, 497. doi:10.2136/sssaj2003.4970
763 Turner, B.L., Newman, S., Newman, J.M., 2006. Organic Phosphorus Sequestration in
764 Subtropical Treatment Wetlands. Environ. Sci. Technol. 40, 727–733.
765 doi:10.1021/es0516256
766 U.S. EPA, 9/99. Field Sampling Guidance Document: Sediment Sampling (No. #1215). U.S.
767 Environmental Protection Agency. Region 9 Laboratory, Richmond California.
768 Vetter, Y.A., Deming, J.W., Jumars, P.A., Krieger-Brockett, B.B., 1998. A Predictive Model of
769 Bacterial Foraging by Means of Freely Released Extracellular Enzymes. Microb. Ecol.
770 36, 75–92. doi:10.1007/s002489900095
771 Viollier, E., Inglett, P.., Hunter, K., Roychoudhury, A.., Van Cappellen, P., 2000. The ferrozine
772 method revisited: Fe(II)/Fe(III) determination in natural waters. Appl. Geochem. 15,
773 785–790. doi:10.1016/S0883-2927(99)00097-9

Biogeosciences Discuss., doi:10.5194/bg-2016-533, 2017
Manuscript under review for journal Biogeosciences
Published: 9 January 2017

774 Wentzel, M.C., Lötter, L.H., Ekama, G.A., Loewenthal, R.E., Marais, G. v R., 1991. Evaluation
775 of Biochemical Models for Biological Excess Phosphorus Removal. Water Sci. Technol.
776 23, 567–576.
777 Yamamoto-Ikemoto, R., Matsui, S., Komori, T., 1994. Ecological interactions among
778 denitrification, poly-P accumulation, sulfate reduction, and filamentous sulfur bacteria in
779 activated sludge. Water Sci. Technol. 30, 201–210.
780

781 ## Figures

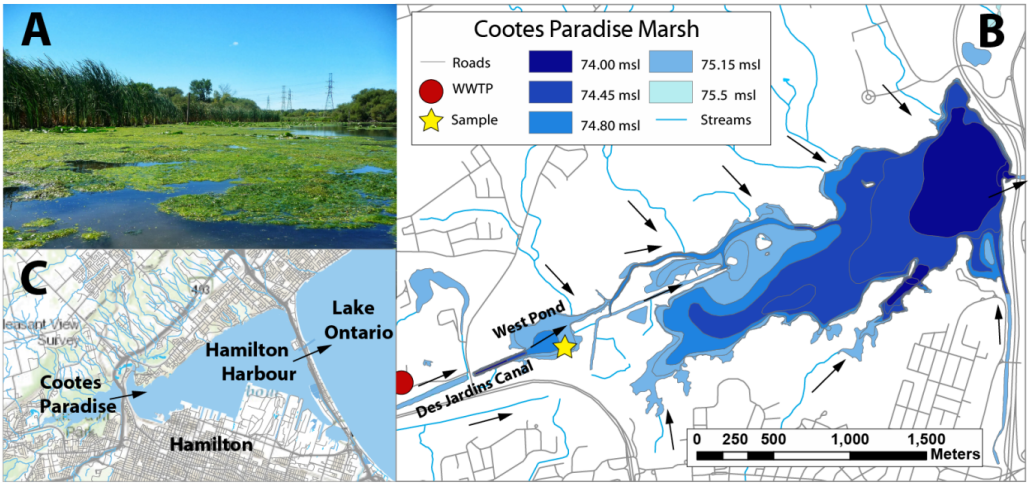

782

783 *Figure 1: A) Photograph of the sampling location taken on the day of sampling*
784 *illustrating the abundance of green filamentous algae. B) Map of Cootes Paradise*
785 *and West Pond showing the sampling location, local hydrological network and the*
786 *King Street Waste Water Treatment plant in Dundas. Color represents area*
787 *covered by surface water at different water levels (msl= meters above sea level)*
788 *C) Overview map showing the hydrological connection between Cootes Paradise,*
789 *Hamilton Harbour and Lake Ontario.*

Biogeosciences Discuss., doi:10.5194/bg-2016-533, 2017
Manuscript under review for journal Biogeosciences
Published: 9 January 2017

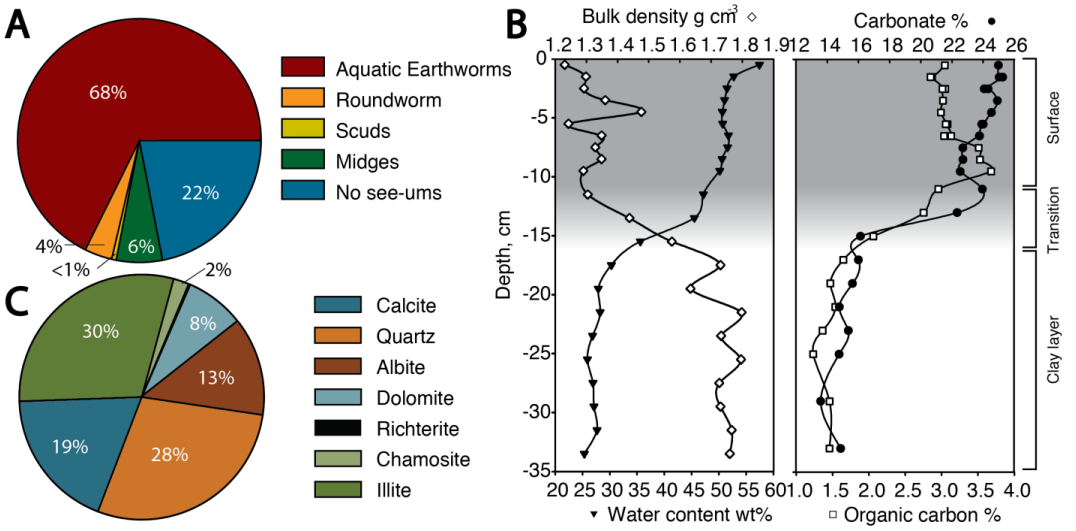

Figure 2: a) Proportions of bioturbating macro invertebrates identified in the top 18 cm b) Depth profiles of sampled sediment, water content weight % (inverted black triangles), bulk density (white diamonds) OM % (white squares), carbonate % (black circles) c) Mineralogical composition of sediments from the zone of bioturbation determined by XRD (top 12 cm).

Biogeosciences Discuss., doi:10.5194/bg-2016-533, 2017
Manuscript under review for journal Biogeosciences
Published: 9 January 2017

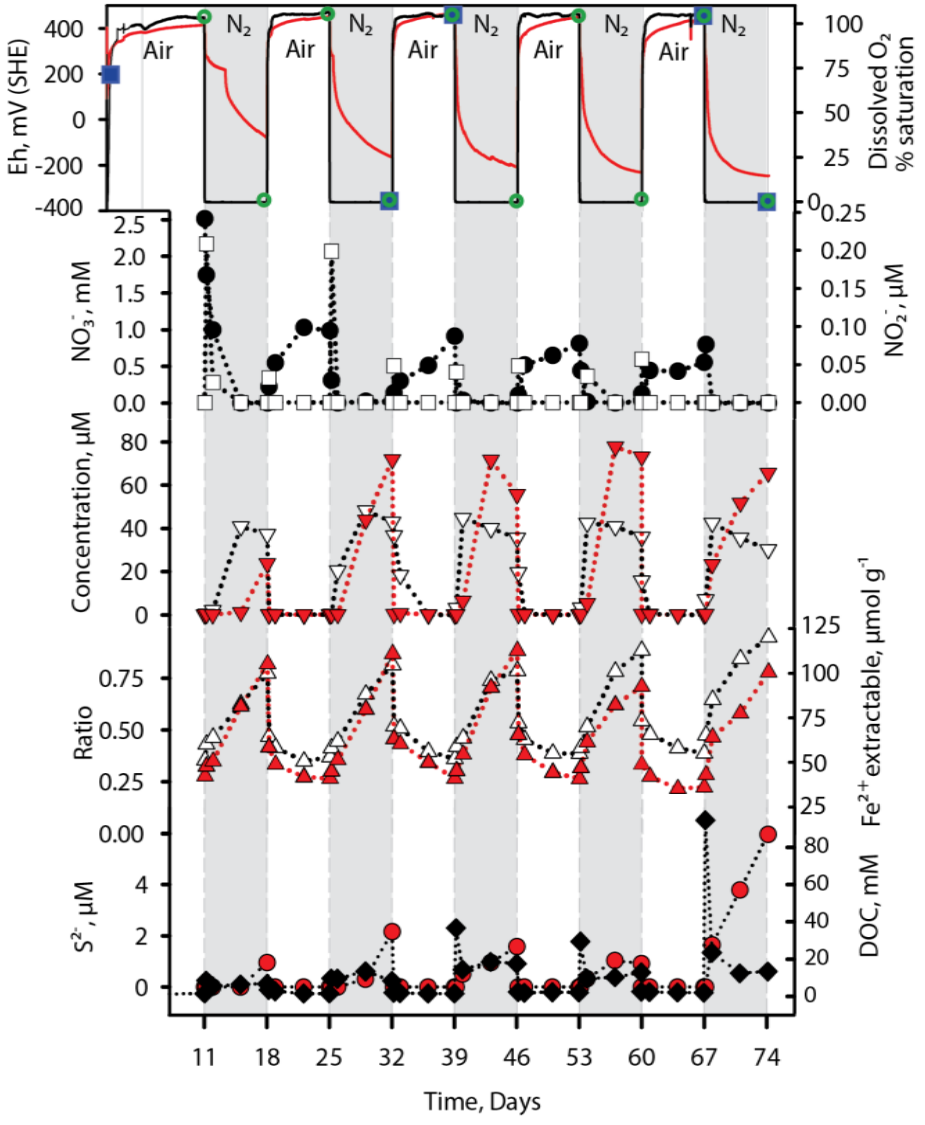

796

797 *Figure 3: Aqueous chemistry and iron extraction data with time during reactor*
798 *experiments: Solid red line = E_h, solid black line = DO, full black circles = NO_3^-,*
799 *white squares = NO_2^-, inverted red triangles = $Fe_{(aq)}$, inverted white triangles =*
800 *$Mn_{(aq)}$, red triangles = Fe^{2+} 0.5M HCl extractable, white triangles = Fe^{2+}/Fe^{3+} ratio*
801 *in 0.5M HCl extract, red circles = S_2^-, black diamonds = DOC. Sampling points for*

Biogeosciences Discuss., doi:10.5194/bg-2016-533, 2017
Manuscript under review for journal Biogeosciences
Published: 9 January 2017

802 *^{31}P NMR and extracellular enzyme assays (EEA) are shown on the E_h curve (^{31}P*

803 *NMR = open blue squares, EEA = open green circles).*

Biogeosciences Discuss., doi:10.5194/bg-2016-533, 2017
Manuscript under review for journal Biogeosciences
Published: 9 January 2017

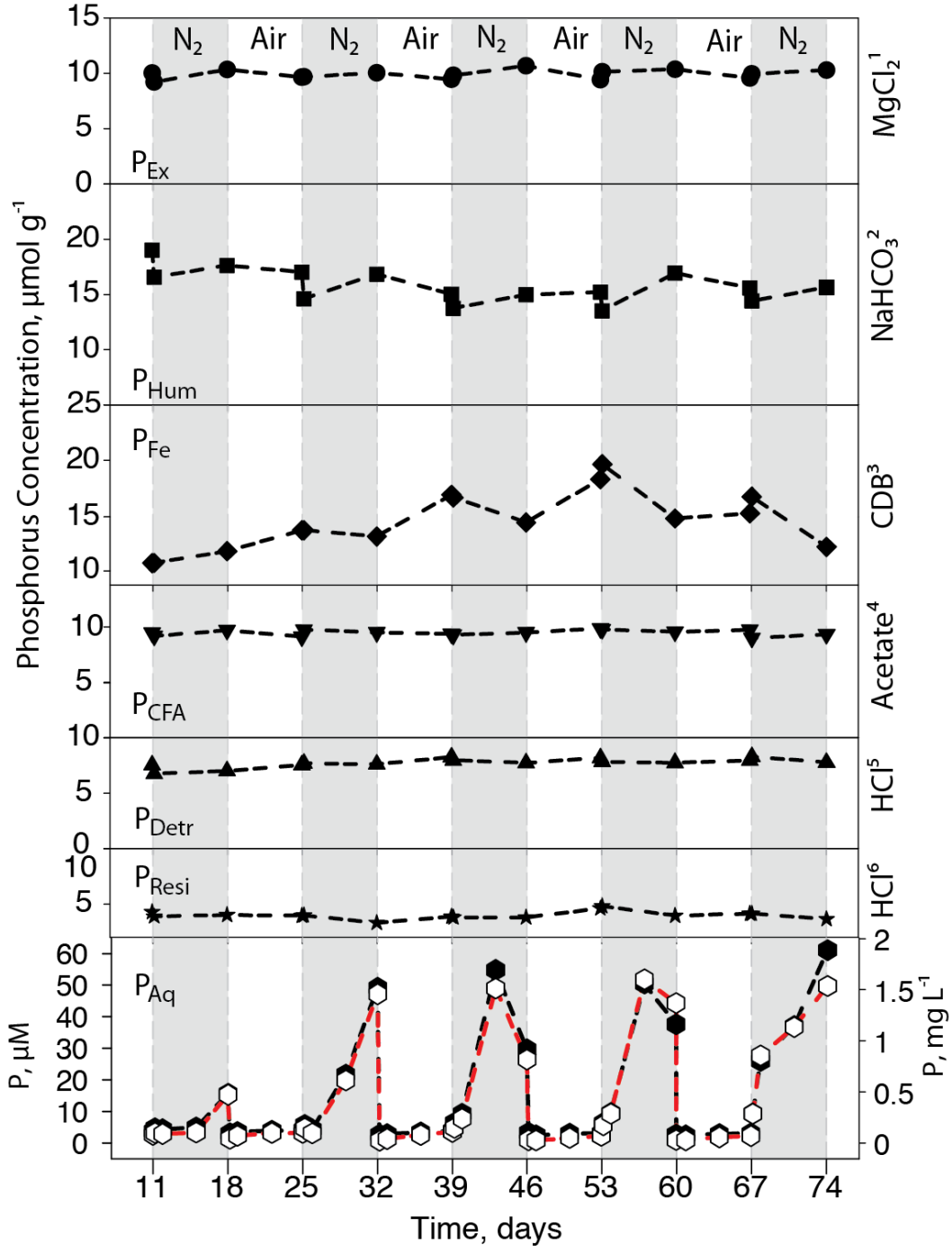

Figure 4: Aqueous and solid phase phosphorus speciation from sequential

Biogeosciences Discuss., doi:10.5194/bg-2016-533, 2017
Manuscript under review for journal Biogeosciences
Published: 9 January 2017

806 *chemical extractions with time during the reactor experiment. White panels*
807 *correspond to time periods with air sparging, grey panels correspond to time*
808 *periods with N_2:CO_2 sparging. Black symbols = total P concentration, white*
809 *symbols = SRP concentration.*

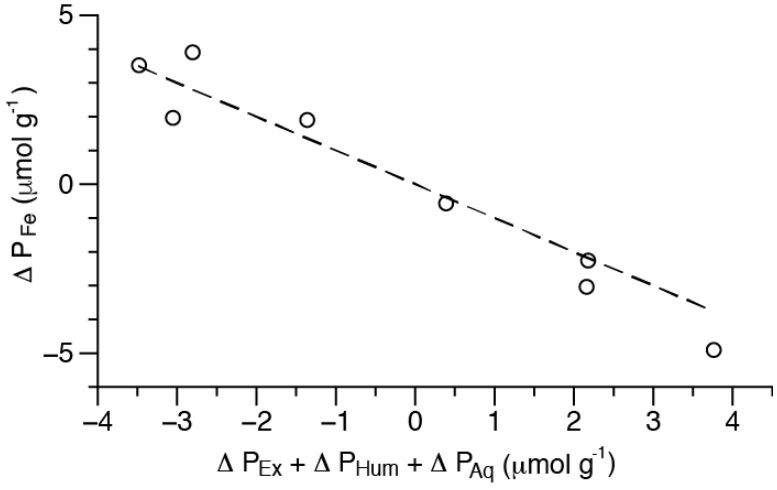

810

811 *Figure 5: Change in P distribution between the start and end of each oxic and*
812 *anoxic period (7 day change). Iron-bound P (P_{Fe}) appears to be reversibly*
813 *redistributed to the loosely sorbed (P_{Ex}), humic bound (P_{Hum}) and aqueous*
814 *fractions (P_{Aq}). The dashed line is 1:1. Linear regression of the data results in an*
815 *R^2 of 0.95, a slope of -1.1 and $p < 0.0001$).*

Biogeosciences Discuss., doi:10.5194/bg-2016-533, 2017
Manuscript under review for journal Biogeosciences
Published: 9 January 2017

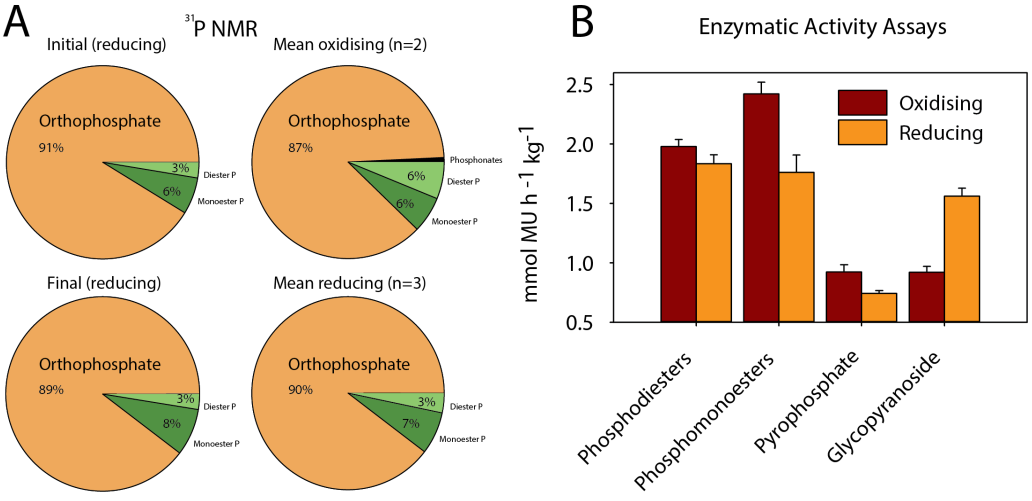

Figure 6: A) P speciation determined by ^{31}P NMR for the initial suspension (top left), the final suspension (bottom left), the average of samples from oxic conditions n=2 (top right), the average of samples from anoxic conditions n=3 (bottom right) B) Average extracellular enzyme activities under oxic and anoxic conditions for MUP, DiMUP, PYRO-P and MUGb (n=5)